

# Rapid fabrication and characterization of MEMS Parylene C bellows for large deflection applications

H M Gensler<sup>1</sup> and E Meng<sup>1,2</sup>

<sup>1</sup> Department of Biomedical Engineering, Viterbi School of Engineering, University of Southern California, 1042 Downey Way, DRB-140, Los Angeles, CA 90089-1111, USA

<sup>2</sup> Ming Hsieh Department of Electrical Engineering, University of Southern California, 3740 McClintock Avenue, EEB-100, Los Angeles, CA 90089-2560, USA

E-mail: [ellis.meng@usc.edu](mailto:ellis.meng@usc.edu)

Received 13 July 2012, in final form 27 August 2012

Published 11 October 2012

Online at [stacks.iop.org/JMM/22/115031](http://stacks.iop.org/JMM/22/115031)

## Abstract

We present a rapid, high-yield fabrication process for Parylene C microbellows for large deflection applications and their characterization. Bellows having different convolution number, wall thickness, inner diameter and outer diameter and layer height were fabricated using a lost wax-like process. The effect of design parameters on overall bellows performance was evaluated through load–deflection testing and finite element modeling (FEM) simulations. Large deflection ( $\sim$ mm) was achieved under relatively low applied pressure ( $\sim$ kPa). The onset of bellows hysteresis (4.19 kPa or 0.60 psi) was determined in mechanical testing and approximated by FEM. For the bellows tested, convolution number, wall thickness and outer diameter had the greatest impact on load–deflection (axial extension) performance. Demonstration of bellows for fluid pumping was achieved through integration with electrochemical actuators operated under low power ( $\sim$ 3 mW). Combined with the biocompatibility, chemical inertness and low permeability of Parylene C, microelectromechanical systems (MEMS) bellows have the potential to enable novel applications in MEMS actuators and microfluidic systems.

(Some figures may appear in colour only in the online journal)

## 1. Introduction

A bellows is a thin-walled corrugated tube [1] typically used as a pressure-responsive device (switch, gauge), flexible shaft coupling, or as a hermetic housing [2]. Miniature metal and ceramic bellows have been employed extensively in many applications, but often require large driving pressures ( $>$ MPa) to produce only modest deflections (tens of microns) due to the relatively high Young's modulus of the materials [3]. A polymer bellows typically has a Young's modulus orders of magnitude less than those of metal and ceramic bellows; thus they require lower pressure (and thus less power) to achieve larger deflections than metal or ceramic bellows. Applications of polymer bellows include electrostatic actuators [4], endoscopic pressure sensors [5], microfluidic channel connectors [6], fuel cell reservoirs [7], piston

actuators [8], pneumatic artificial rubber muscles [9], bending pneumatic actuators [10] and electrochemical actuators [11, 12].

Microelectromechanical systems (MEMS) bellows made of nonpolymer materials [3] have been produced using surface micromachining in which alternating layers of structural and sacrificial materials are deposited and patterned until the final stacked multiconvolution structure is achieved. However, the layer-by-layer nature of the process is time consuming and impractical for producing polymer bellows having more than a few convolutions. MEMS polymer bellows have generally been fabricated using an alternate process in which a sacrificial bellows template is first produced using a microfabricated mold. The template is then coated with the desired polymer and the sacrificial material removed to release the polymer bellows structure. Mold features from  $\mu$ m to mm can be achieved by

**Table 1.** MEMS fabrication techniques for polymer bellows.

Fabrication	Sacrificial material	Bellows material	Application	Dimensions	Operation range	Ref.
<i>Mold patterning via subtractive process</i>						
Excimer laser ablation (PI mold), oblique evaporation (Au), vapor deposition (Parylene)	Polyimide, brass	Parylene C-gold-Parylene C-gold	Electrostatic actuator	1.2 mm diameter, ~900 $\mu\text{m}$ L, 23 $\mu\text{m}$ thread pitch	NA	[4]
<i>Mold patterning via additive process</i>						
Sacrificial wax molding, vapor deposition	Wax (not specified)	Parylene C	Microfluidic channel connectors	NA	NA	[6]
Stereolithography, sacrificial wax molding, vapor deposition	Wax (not specified)	Parylene C-PDMS-Parylene C	Fuel cell delivery systems reservoir	~100 $\mu\text{m}$ total wall thickness; 10 mm OD $\times$ 12.7 L; 15.7 mm L	44.8 kPa (linear design), 13.8 kPa (rotary design)	[7]
Sacrificial PDMS and wax molding; vapor deposition	PDMS, PEG	Parylene C	Electrochemical actuator	6 mm ID $\times$ 9 mm OD; 10 $\mu\text{m}$ thick	up to ~12 kPa	[11]
Reusable PDMS and sacrificial wax molding; vapor deposition	PEG	Parylene C	Drug delivery device actuator	6 mm ID $\times$ 9 mm OD; 13.5 $\mu\text{m}$ thick	up to 3.45 kPa	[12]
Reusable PDMS and sacrificial wax molding; vapor deposition	PEG	Parylene C	Electrochemical actuator	Varies with design, see table 3	up to 3.45 kPa; higher for burst testing	This work
<i>Direct fabrication of bellows via additive process</i>						
Focused-ion-beam chemical vapor deposition (FIB-CVD)	None	Phenanthrene	Demonstrate FIB-CVD fabrication method	0.8 $\mu\text{m}$ pitch, 0.1 $\mu\text{m}$ thickness, 2.75 $\mu\text{m}$ OD, 6.1 $\mu\text{m}$ H	NA	[13]

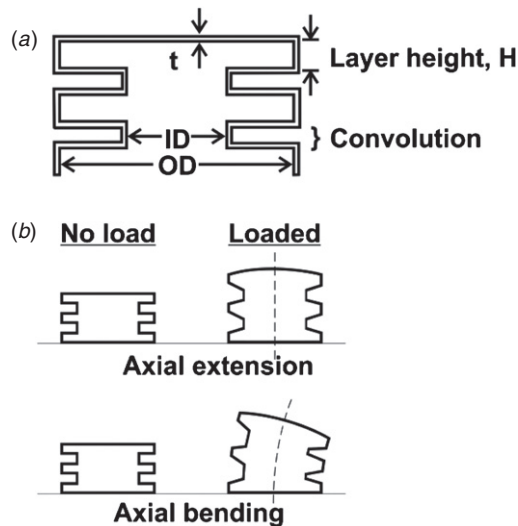
NA = information not available.

either subtractive or additive MEMS processes. A brief survey of recent work in fabrication of MEMS polymer bellows is given in table 1 and is grouped according to the manner in which the template molds were produced.

Minami *et al* [4] used subtractive laser ablation for mold generation paired with metal oblique evaporation and Parylene deposition to fabricate a composite metal–polymer bellows for application in an electrostatic actuator. Although resolution of this subtractive process was relatively high (23  $\mu\text{m}$ ), the process required multiple intermediate sacrificial materials that were not reusable and was time consuming due to the serial nature of producing the laser ablated molds. In additive processes [6, 7, 11–13], molds are constructed in a bottom-up approach. Luharuka *et al* [7] fabricated bellows for storage reservoirs in a fuel delivery system. Stereolithography (SLA) negative molds achieved 50  $\mu\text{m}$  minimum features but subsequent processing steps limited the final part's minimum feature size to 0.5 mm. Wax impressions formed with the SLA molds were coated with Parylene. The wax was then removed with boiling borax and a brush-coat of PDMS was applied to the Parylene bellows for structural strength. Boiling, if using a high melting temperature wax, could induce thermal stress on the Parylene and contamination with borax is undesirable for *in vivo* applications. Feng *et al* [6] presented a room

temperature sacrificial wax molding technique for Parylene bellows, but also required a non-biocompatible solvent to remove the wax, which induced residual stress in the Parylene. Although submicron resolution is possible, current additive methods are limited by the use of expensive equipment, to select materials, or by low throughput. Finally, the production of bellows-like structures directly by focused-ion-beam chemical vapor deposition (FIB-CVD) was reported with submicron feature sizes [13], but at the cost of long exposure time and was limited to phenanthrene. Extrapolating to a 1 mm high structure, fabrication would require over 13 h.

Of these methods, a sacrificial wax process is attractive as it does not require specialized equipment and can be relatively low cost. Our group previously developed a sacrificial molding technique utilizing polyethylene glycol (PEG) for MEMS electrochemically driven bellows actuators for drug delivery. The actuator consisted of a Parylene bellows filled with electrolyte (water) and attached to platinum interdigitated electrodes [11, 14]. The bellows shape was chosen over corrugated or flat membranes because it can achieve higher deflection (in simulations, 1.5 mm for bellows versus 0.8 mm for corrugated diaphragm of similar dimensions) with less applied pressure [11]. When activated, the actuator pumped drug out of an adjacent reservoir. PEG was selected as the



**Figure 1.** (a) Standard profile of a bellows with design parameters labeled. (b) Application of load to a bellows results in axial extension, axial bending or a combination thereof.

template for its biocompatibility and ability to dissolve in warm water. However, only a 1.5 convolution bellows was achieved, and the fabrication process of bellows was time intensive and had low yield. To foster new applications with MEMS bellows, fabrication needs to progress from serial to parallel or batch production, molds should be reusable or inexpensive, the molding step should not stress the polymer and the intermediate sacrificial materials should not pose a contamination concern when the bellows are integrated with microfluidic systems.

Here, we report a new rapid high-yield fabrication process for polymer bellows and characterization of five bellows design parameters using mechanical load–deflection testing and finite element models. Preliminary results on a limited number of bellows designs were presented in [15]. The new nonlithography-based process reduces fabrication time (1 week down to 1 day) features reusable molds, does not require expensive equipment, utilizes wax that is water soluble at room temperature and achieves higher yields in contrast to [11]. To the best of our knowledge, this work presents the first study of polymer bellows design parameters and their effects on axial extension.

## 2. Bellows modeling

A standard profile of a bellows fixed at one end is shown in figure 1, where  $t$  is the wall thickness, ID the inner diameter of the bellows, OD the outer diameter of the bellows and  $H$  the height of one layer. The number of convolutions will be referred to as  $N$ . As shown in figure 1, under applied loads, and assuming no twisting, bellows undergo axial extension (the focus of this work), axial bending or a combination thereof.

Metal and ceramic bellows are typically treated as a series of stacked diaphragms (or plates) [2], each of which behaves according to classical plate theory as they undergo small deflection relative to the diaphragm thickness. The total bellows deflection is the sum of the individual diaphragm

**Table 2.** Finite element model material properties and bellows dimensions.

Dimension	Value
Wall thickness ( $\mu\text{m}$ )	13.5
Inner diameter (mm)	6
Outer diameter (mm)	9
Layer height (mm)	0.4
Number of convolutions	1, 2, and 3
Material properties	Value
Young's modulus (GPa)	2.76
Tensile strength (MPa)	68.9
Yield strength (MPa)	55.2
Poisson's ratio	0.40
Density ( $\text{g cm}^{-3}$ )	1.289

deflections and can be approximated using linear analytical models. Thin polymer bellows, which exhibit highly nonlinear behavior, violate the assumption of small or moderately large deflection and are not adequately described by diaphragm or even thin diaphragm (membrane) theory. Due to the complex geometry of the bellows and highly nonlinear behavior of thin polymers, an analytical closed-form solution is impractical [16] and instead finite element modeling (FEM) can be employed to model deflection and stress under various loads. FEM has previously been used for characterization and modeling of complex polymer structures, such as in [17, 18].

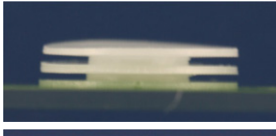



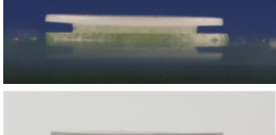

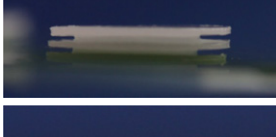
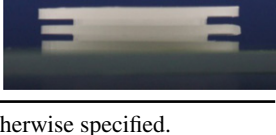
Three-dimensional finite element models were developed for nonlinear static simulations (Solidworks Simulation 2010, Dassault Systèmes SolidWorks Corp., Concord, MA) of three bellows designs (varying number of convolutions). Quarter models were used given the geometric symmetry and to minimize processing time. The large displacement formulation and direct sparse solver were used to account for the highly nonlinear nature of the polymer bellows. Loads from 0.00 kPa to 3.45 kPa (0.50 psi, 25.86 mmHg) were applied and the resulting deflection and von Mises stress values were recorded. Material properties and dimensions used for the finite element models are shown in table 2.

## 3. Design and fabrication

Chlorinated poly(para-xylylene), or Parylene C, was chosen as the material for the bellows for its ability to be vapor deposited at room temperature, low permeability to gases and liquids, low Young's modulus (2.76 GPa (manufacturer) to 4.75 GPa [19]), biocompatibility (USP Class VI and ISO 10993) and inertness to a broad range of chemicals (no known solvents at room temperature).

Bellows were made with varying dimensions in order to evaluate the effect of design parameters (wall thickness, inner diameter, outer diameter, layer height, number of convolutions) on overall bellows performance. The inner and outer bellows diameters were chosen to correspond with the active area of the electrochemical actuator, in which bellows utility was demonstrated. Bellows overall height was intentionally kept low to minimize profile. The bellows wall thickness was varied in order to determine the appropriate thickness for robustness and to evaluate the effect of thickness

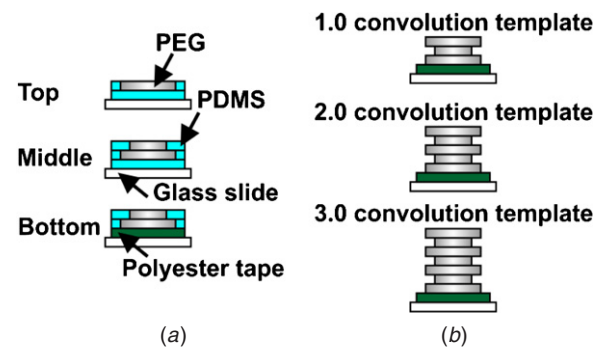
**Table 3.** Summary of the fabricated bellows designs.

Dimensions <sup>a</sup> (ID–OD– <i>H</i> )	Number of convolutions	ID/OD	Parylene-coated PEG template
5–10–0.4	2	0.50	
5–9–0.4	2	0.56	
6–9–0.4	3	0.67	
6–9–0.4	2	0.67	
6–9–0.4	1	0.67	
6–9–0.4 (15.5 $\mu\text{m}$ )	2	0.67	
6–9–0.3	2	0.67	
7–10–0.4	2	0.70	

<sup>a</sup> All wall thicknesses 13.5  $\mu\text{m}$  unless otherwise specified.

on deflection. Each bellows design is shown in table 3 along with its inner to outer diameter ratio. The naming convention used for designs was as follows: ID–OD–*H*, *N*, *t*. Thus, 6–9–0.4, 2, 13.5 describes a bellows with inner diameter of 6 mm, outer diameter of 9 mm, layer height of 0.4 mm, 2 convolutions and a wall thickness of 13.5  $\mu\text{m}$ .

Fabrication of the bellows consisted of a two part molding process (figure 2). First, a set of reusable polydimethylsiloxane (PDMS, Sylgard 184; Dow Corning Corp., Midland, MI) sheets were made of a specified thickness (0.3 and 0.4 mm) using a custom frame of brass shims (Precision Brand, Downers Grove, IL) mounted to a flat glass plate (Nanofilm, Westlake Village, CA). Uncured PDMS was poured into the frame and excess removed with a squeegee. After curing in an oven at 80 °C for 1 h, the PDMS sheet was cut into 15 × 15 mm squares. Perforations equal to the dimensions of the inner or outer diameters of the bellows were made in the center of the PDMS squares using metal arch punches (C.S. Osborne & Co., Harrison, NJ). The edges of the metal punches were polished

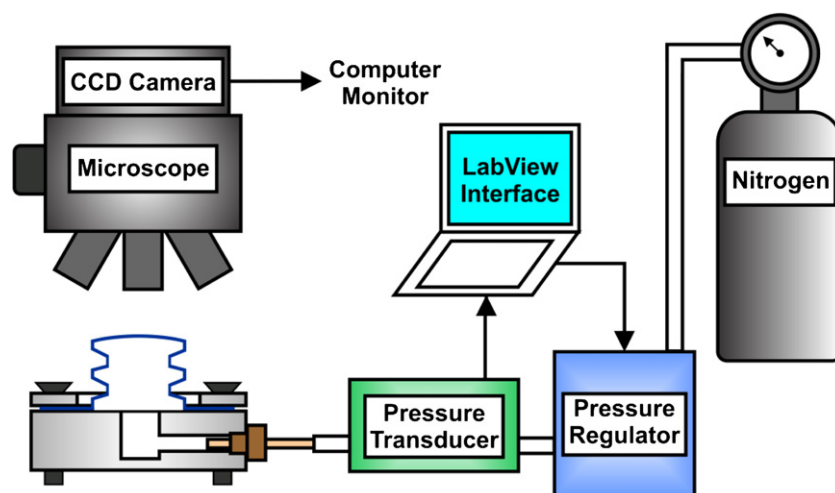


**Figure 2.** Two part molding process for fabrication of bellows. (a) Three modules of PEG-filled PDMS molding sheets with punched holes were used in various combinations to rapidly form any desired number of convolutions, and then PEG forms acted as (b) a sacrificial template for Parylene C coating.

with ultrafine sandpaper to improve smoothness of the cut. The sheets were visually aligned (horizontal alignment within  $\sim 50 \mu\text{m}$  with use of a microscope) and stacked as shown in figure 2 to form three different modules. Alignment of PDMS molding sheets for a dozen bellows required less than 1 h. Glass slides served as the base substrate for stacking. Polyester tape (8403; 3M, St. Paul, MN) placed below the PDMS stack facilitated removal of bellows after Parylene coating. Middle and top modules included an additional flat solid sheet of PDMS to facilitate transfer of the modules during stacking. The number of convolutions was increased by adding additional middle modules.

The reusable modules were filled with molten (50 °C) low molecular weight ( $M_n$  1000) polyethylene glycol (PEG; Alfa Aesar, Ward Hill, MA). With lower molecular weight PEG (1000 instead of 14 000) smoother and less brittle replicas were obtained upon cooling than in [11]. In addition, the lower melting temperature of the PEG 1000 eliminated the need for vacuuming and mold reinforcement as described in [11], which was used to prevent the molten PEG from leaking between the stacked PDMS molding sheets. PEG 1000 did not leak between our PDMS sheets as long as the temperature was kept below 60 °C. Removing the reinforcement step saved time during the mold preparation steps and allowed reuse of molding sheets, such that total fabrication time was reduced from 1 week to 1 day. Solidified PEG templates, consisting of one or two layers each as shown in figure 2, were stacked and fused by moistening the opposing faces of the modules to create bellows templates in increments of 1 convolution. Bellows templates (1, 2, or 3 convolutions) were coated with 13.5 or 15.5  $\mu\text{m}$  of Parylene C (PDS 2010; Specialty Coating Systems, Indianapolis, IN), after which the sacrificial PEG was removed by soaking in room-temperature deionized water. This new improved fabrication process of bellows features reusable molds, does not induce thermal stress in the bellows material, uses a sacrificial material that is available in biocompatible formulations, achieves yields of up to 90% and takes only 1 day.





**Figure 3.** Load–deflection testing of the bellows. Nitrogen supply was regulated to obtain discrete pressures and a compound microscope ( $100\times$  objective,  $1\text{ }\mu\text{m}$  vertical resolution) was used to measure deflection.

## 4. Experimental methods

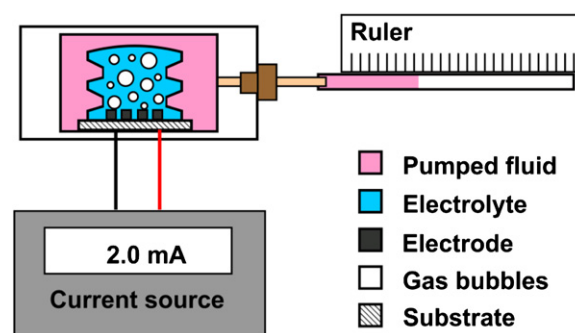
### 4.1. Mechanical characterization

Bellows were clamped in a custom acrylic test fixture connected to a custom pressure setup (figure 3). An electronic pressure regulator (900X; ControlAir Inc., Amherst, NH) controlled using a LabView (National Instruments, Austin, TX) interface regulated nitrogen supplied from a pressurized nitrogen gas cylinder. Loads were applied at room temperature to the bellows mounted in the fixture and deflection of the center of the top of the bellows was recorded using a compound microscope (PSM-1000; Motic China Group Co., Xiamen, China) with a  $100\times$  objective lens. The fine focus knob has a calibrated resolution of  $1\text{ }\mu\text{m}$  per division. The center point of the bellows top surface was brought into focus under no load, then refocused under loading to determine the deflection in microns based on the number of divisions. To minimize backlash, the knob was continually adjusted in one direction only. Verification with a pressure calibrator mounted at the test fixture outlet ensured that delays were minimal ( $<5\text{ s}$ ) between the pressure measured at the regulator and at the test fixture.

For mechanical characterization in the elastic range, loads from  $0.00\text{ kPa}$  to  $3.45\text{ kPa}$  ( $25.86\text{ mmHg}$ ,  $0.50\text{ psi}$ ) were applied in discrete steps of  $0.69\text{ kPa}$  every  $2\text{ min}$ . The onset of plastic deformation was determined by load cycling to successively higher pressures until hysteresis of the deflection curve was observed. Between each load cycle, the bellows was left unloaded for approximately  $15\text{ min}$  to observe relaxation. Load cycling was previously used to characterize flat Parylene C membranes [19]. Burst pressure (ultimate tensile strength) was evaluated by increasing pressure until the bellows burst or leaked.

### 4.2. Demonstration in an electrochemical actuator

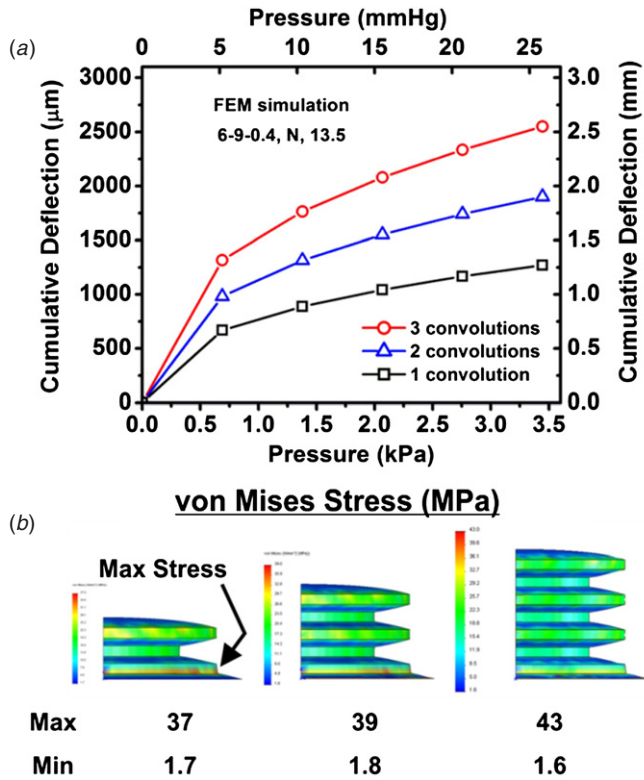
Bellows were integrated with electrochemical actuators as described in [12, 20]. Platinum electrodes with a titanium adhesion layer were fabricated on a glass substrate with a dual-layer photolithography and liftoff process, after which



**Figure 4.** Bellows integrated with MEMS electrochemical actuators were mounted in a reservoir for flow rate testing.

they were coated with Nafion<sup>®</sup> [20]. Bellows were filled with electrolyte (water) and assembled onto electrodes using the double-sided pressure sensitive adhesive film (3M<sup>™</sup> Double Coated Tape 415, 3M, St. Paul, MN) and reinforced with marine epoxy (Loctite; Henkel Corp., Rocky Hill, CT) to form bellows electrochemical actuators (BEA). Kynar<sup>™</sup> wire-wrap wires (30 AWG; Jameco Electronics, Belmont, CA) were attached to the electrodes with silver epoxy (EPO-TEK<sup>®</sup> H20E, Epoxy Technology, Inc., Billerica, MA) and further insulated with marine epoxy.

Acrylic reservoirs were custom machined and the BEA placed within for flow rate testing at room temperature (figure 4). Constant current of  $2.0$  or  $5.0\text{ mA}$  was applied (2400 Sourcemeter; Keithley Instruments Inc., Cleveland, OH) to the wires of the BEA to induce electrolysis within the bellows. The phase changed-induced pressure increase extended the bellows and applied pressure to reservoir fluid surrounding the bellows to force fluid out of the reservoir. Flow rates and volumes were measured by a calibrated micropipette ( $100\text{ }\mu\text{L}$ ; VWR International, Radnor, PA) attached at the outlet. Note that in contrast to the pressure setup, in which pressure was applied to a closed system and held at static pressure values, the integrated reservoir system is open (via the cannula outlet) and the pressure values were dynamic.



**Figure 5.** Finite element model simulation of (a) deflection and (b) von Mises stress for bellows with 1, 2 and 3 convolutions, but all other parameters constant (6 mm ID, 9 mm OD, 0.4 mm  $H$ , 13.5  $\mu\text{m}$  wall thickness).

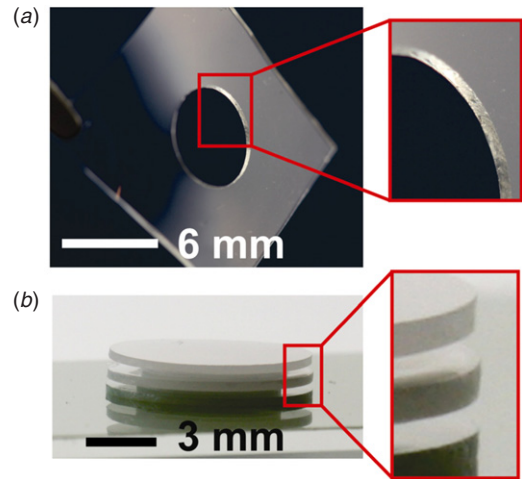
#### 4.3. Statistical analysis

Each of the bellows design parameters (outer diameter, inner diameter, wall thickness, layer height, number of convolutions) was subjected to a two-tailed  $t$ -test for two independent samples with unequal variances. For load–deflection testing, each sample consisted of three bellows of the same design tested three times. For flow rate testing, three measurements were made for each bellows design at each applied current value.

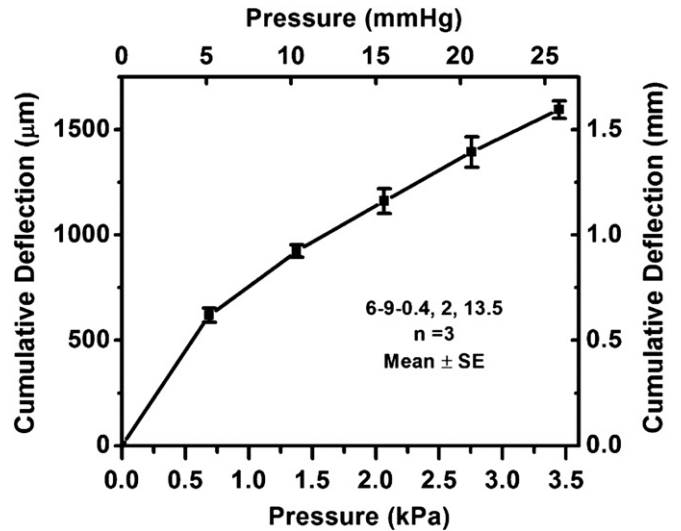
## 5. Results

### 5.1. Finite element model simulations

The resulting curves for 3D nonlinear static FEM deflection simulations (figure 5) showed that the yield stress of Parylene (55.2 MPa according to the manufacturer and 59 MPa according to [19]) was not exceeded at 3.45 kPa, the maximum pressure applied. The highest stresses were observed at the 90° corners at the base of the bellows (figure 5(b)). The 1 and 2 convolution bellows FEM simulations of deflection were slightly larger but on the same order of magnitude as mechanical testing, but the 3 convolution was noticeably underestimated in the simulation compared to the mechanical results which are discussed in subsequent sections.



**Figure 6.** Photographs of the sidewall of (a) PDMS molding sheet and (b) Parylene C-coated bellows template prior to sacrificial PEG removal.



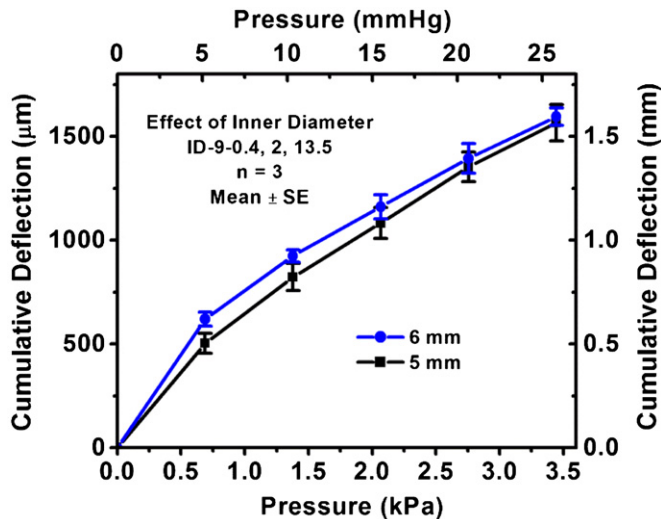
**Figure 7.** Mechanical testing of three identical bellows (6 mm ID, 9 mm OD, 0.4 mm  $H$ , 2 convolutions, 13.5  $\mu\text{m}$  wall thickness) demonstrating uniform performance during load–deflection testing.

### 5.2. Fabrication

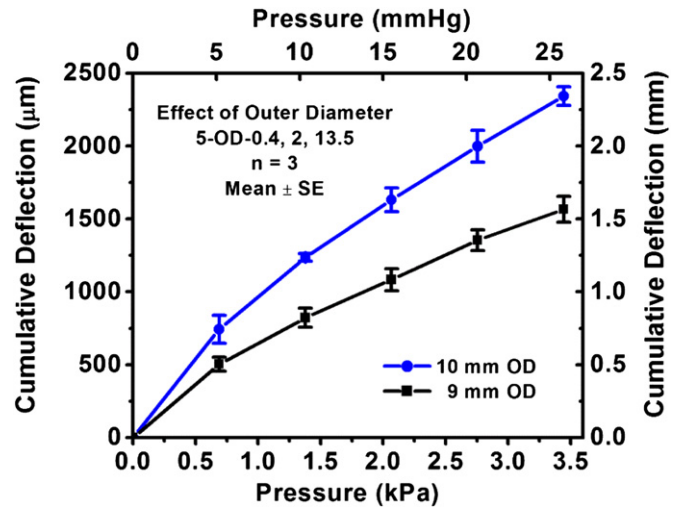
The sidewall profile is determined by the smoothness of the cut into the PDMS. Photographs of the PDMS molding sheet sidewall and the Parylene C-coated PEG sacrificial template are shown in figure 6.

### 5.3. Mechanical characterization

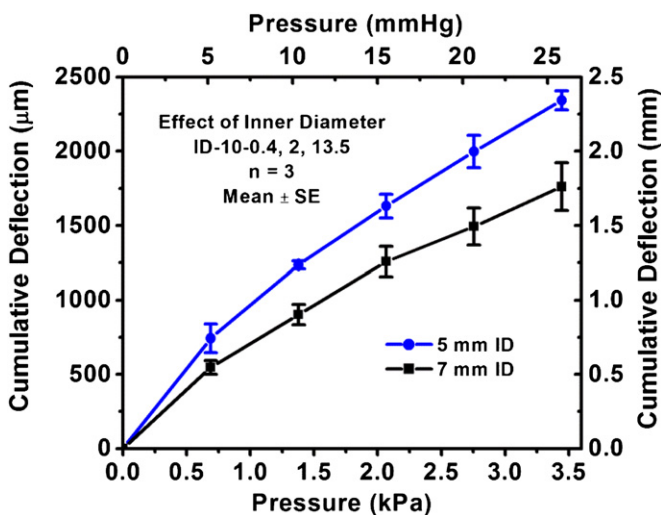
**5.3.1. Repeated loading of individual bellows and uniformity between bellows of same design.** Three bellows of the exact same design were each subjected to the same load–deflection test three times. Individual bellows showed no signs of plastic deformation up to 3.45 kPa for the three cycles. The load–deflection curves of three bellows of the same design were extremely similar. Typically, the standard error for a group of bellows of the same design was 5–10% of the deflection value. As shown in figure 7, the standard error can be as low as 3% (at 3.45 kPa).



**Figure 8.** Mechanical testing of two bellows designs, with inner diameters of 6 and 5 mm, but all other parameters constant (9 mm OD, 0.4 mm  $H$ , 2 convolutions, 13.5  $\mu\text{m}$  wall thickness).



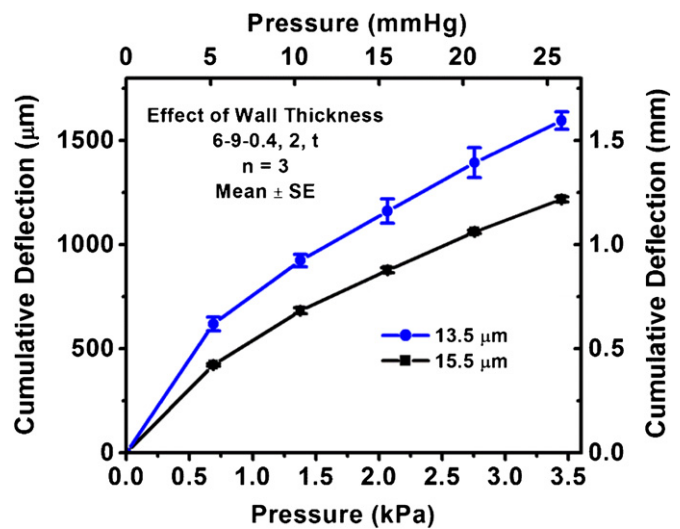
**Figure 10.** Mechanical testing of two bellows designs, with outer diameters of 9 and 10 mm, but all other parameters constant (5 mm ID, 0.4 mm  $H$ , 2 convolutions, 13.5  $\mu\text{m}$  wall thickness).



**Figure 9.** Mechanical testing of two bellows designs, with inner diameters of 5 and 7 mm, but all other parameters constant (10 mm OD, 0.4 mm  $H$ , 2 convolutions, 13.5  $\mu\text{m}$  wall thickness).

**5.3.2. Inner diameter.** The effect of inner diameter was characterized by fabricating a pair of bellows designs in which the inner diameter was decreased by 1 mm and a second pair that differed by 2 mm. All other parameters for a given pair were kept constant. Decreasing the inner diameter from 6 mm to 5 mm while keeping all other design parameters constant did not significantly alter the overall load–deflection curve (figure 8). The results were not significantly different ( $p > 0.05$ ).

Decreasing the inner diameter of the bellows from 7 mm to 5 mm, keeping all other design parameters constant, resulted in increased deflection for all pressures tested (a difference of 581  $\mu\text{m}$  at 3.45 kPa) as shown in figure 9. However, the difference between the two data sets was significant only for 3.45 kPa ( $p < 0.05$ ).



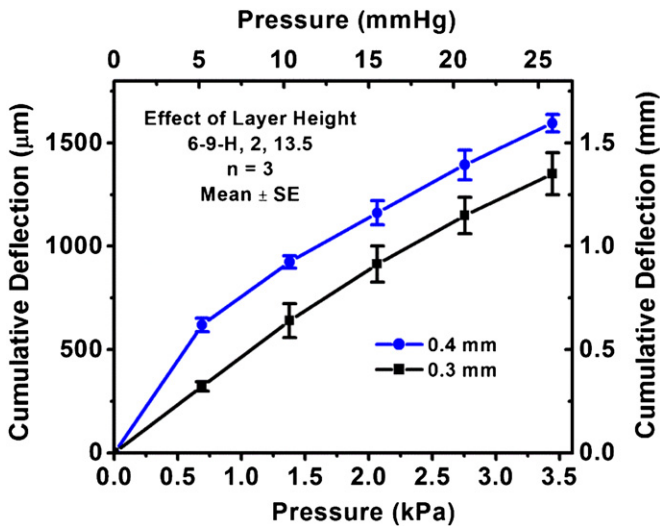
**Figure 11.** Mechanical testing of two bellows designs, with wall thicknesses of 13.5 and 15.5  $\mu\text{m}$ , but all other parameters constant (6 mm ID, 9 mm OD, 0.4 mm  $H$ , 2 convolutions).

**5.3.3. Outer diameter.** Increasing the outer diameter from 9 mm to 10 mm, keeping all other parameters constant, resulted in a significant upward shift in the overall load–deflection curve (figure 10;  $p < 0.05$ ). At 3.45 kPa, the difference in deflection was 776  $\mu\text{m}$ .

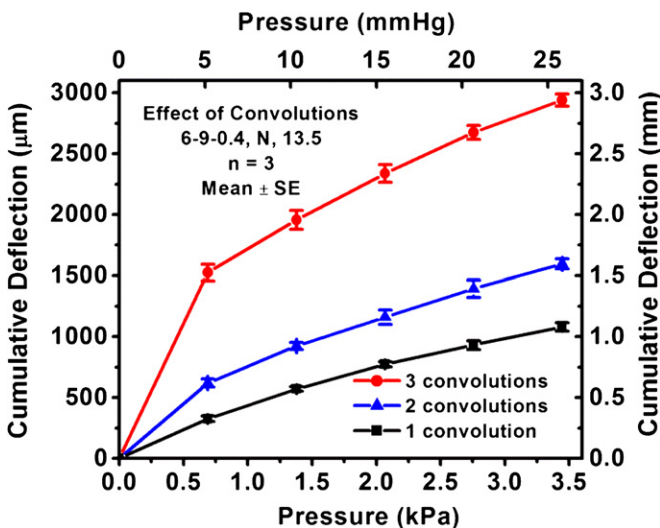
**5.3.4. Wall thickness.** A 2  $\mu\text{m}$  reduction in wall thickness resulted in a significant increase in the overall deflection of a given bellows design (figure 11;  $p < 0.05$ ). At 3.45 kPa the deflections were 1218 and 1595  $\mu\text{m}$  (a difference of 377  $\mu\text{m}$ ) for 15.5 and 13.5  $\mu\text{m}$  wall thicknesses, respectively.

**5.3.5. Layer height.** Increasing the layer height from 0.3 mm to 0.4 mm, keeping all other parameters constant, shifted the overall load–deflection curve at 3.45 kPa upward from 1350 to 1595  $\mu\text{m}$  (245  $\mu\text{m}$ ) as shown in figure 12 ( $p < 0.05$ ).





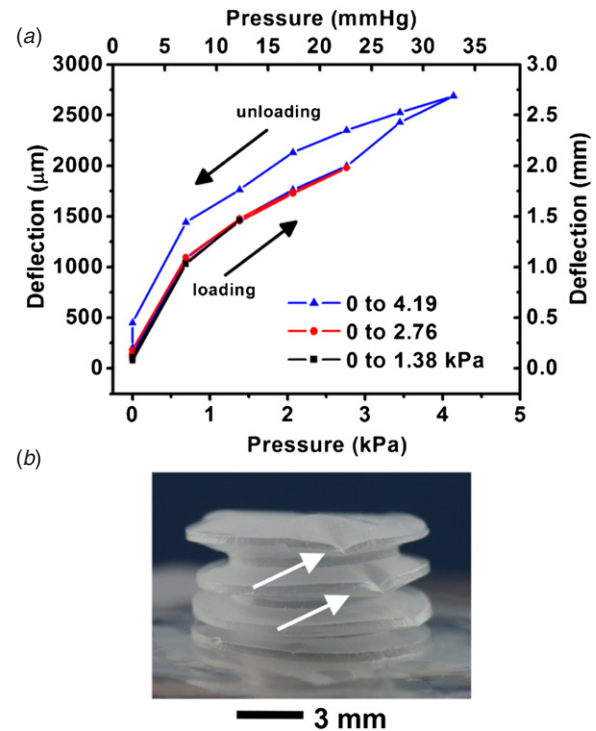
**Figure 12.** Mechanical testing of two bellows designs, with layer heights of 0.3 and 0.4 mm, but all other parameters constant (6 mm ID, 9 mm OD, 2 convolutions, 13.5  $\mu\text{m}$  wall thickness).



**Figure 13.** Mechanical testing of three bellows designs with 1, 2, and 3 convolutions, but all other parameters constant (6 mm ID, 9 mm OD, 0.4 mm  $H$ , 13.5  $\mu\text{m}$  wall thickness).

**5.3.6. Number of convolutions.** Increasing the number of convolutions from 1 to 2 and 2 to 3 resulted in a statistically significant upward shift of the load–deflection curve (figure 13;  $p < 0.05$ ). The shift from 2 to 3 convolutions was noticeably greater (1595–2941  $\mu\text{m}$  at 3.45 kPa) than the shift from 1 to 2 convolutions (1080–1595  $\mu\text{m}$  at 3.45 kPa).

**5.3.7. Summary of load–deflection testing.** The effects of varying the bellows design parameters are summarized in table 4. Entries with a \* indicate statistical significance, as obtained from a  $t$ -test. Decreasing the inner-to-outer diameter (ID/OD) ratio resulted in an increase in overall deflection, but was more effective with an increase in OD rather than a decrease in ID. The wall thickness, layer height and convolution number were varied (individually) and resulted in statistically significant changes in deflection.



**Figure 14.** (a) Hysteresis of the bellows (6 mm ID, 9 mm OD, 0.4 mm  $H$ , 3 convolutions, 13.5  $\mu\text{m}$  wall thickness) upon unloading was observed after load cycling the bellows up to 4.19 kPa (0.6 psi). (b) Above 4.19 kPa, dimpling (arrows) occurred at the outer edges of the convolutions and plastic deformation was observed.

**Table 4.** Summary of the effects of individual bellows design parameters on load–deflection performance.

Parameter	Variation	Effect on deflection at 3.45 kPa
Outer diameter 5–9–0.4 versus 5–10–0.4 (2 convo, 13.5 $\mu\text{m}$ )	Increase 1 mm (11%)	*Increase 776 $\mu\text{m}$ (50%)
Inner diameter 7–10–0.4 versus 5–10–0.4 (2 convo, 13.5 $\mu\text{m}$ )	Decrease 2 mm (29%)	Increase 581 $\mu\text{m}$ (33%)
Wall thickness 15.5 $\mu\text{m}$ versus 13.5 $\mu\text{m}$ (6–9–0.4, 2 convo)	Decrease 2 $\mu\text{m}$ (13%)	*Increase 377 $\mu\text{m}$ (31%)
Layer height 6–9–0.3 versus 6–9–0.4 (2 convo, 13.5 $\mu\text{m}$ )	Increase 0.1 mm (33%)	*Increase 245 $\mu\text{m}$ (18%)
Convolution number 1 versus 2 convo (6–9–0.4, 13.5 $\mu\text{m}$ )	Increase 1 to 2 (100%)	*Increase 515 $\mu\text{m}$ (48%)
Convolution number 2 versus 3 convo (6–9–0.4, 13.5 $\mu\text{m}$ )	Increase 2 to 3 (50%)	*Increase 1345 $\mu\text{m}$ (84%)

\*Statistical significance ( $p < 0.05$ ).

**5.3.8. Elastic range and burst pressure.** The upper limit of the elastic range was determined by load cycling one of the bellows (6–9–0.4, 3, 13.5  $\mu\text{m}$ ) until hysteresis was observed in the load–deflection curve (figure 14). Cycling from 0.00 kPa





**Figure 15.** Photographs of bellows (6 mm ID, 9 mm OD, 0.4 mm  $H$ , 13.5  $\mu\text{m}$  wall thickness) with 1, 2 and 3 convolutions subjected to pressure just below burst pressure and exhibiting plastic deformation.

**Table 5.** Summary of burst pressures for the various bellows designs.

Dimensions ID–OD– $H$ (mm)	Number of convolutions	ID/OD	Burst pressure (kPa)
5–10–0.4	2	0.50	83
5–9–0.4	2	0.56	96
6–10–0.4	2	0.60	61
6–9–0.4	3	0.67	>100
6–9–0.4 (15.5 $\mu\text{m}$ )	2	0.67	>100
6–9–0.4	2	0.67	>100
6–9–0.4	1	0.67	>100
6–9–0.3	2	0.67	>100
7–10–0.4	2	0.70	65

to 1.38 kPa and 0.00 kPa to 2.76 kPa (0.00–0.20 psi and 0.00–0.40 psi) showed negligible hysteresis between loading and unloading. Noticeable hysteresis was observed upon unloading during testing over the span of 0.00–4.19 kPa (0.00–0.60 psi). A waiting period between cycles (on the order of 10 min) allowed the bellows to return to the starting unloaded position. A loading cycle up to 5.52 kPa (0.80 psi) resulted in significant dimpling at the outer edge of the convolutions (figure 14), and plastic deformation was observed after unloading.

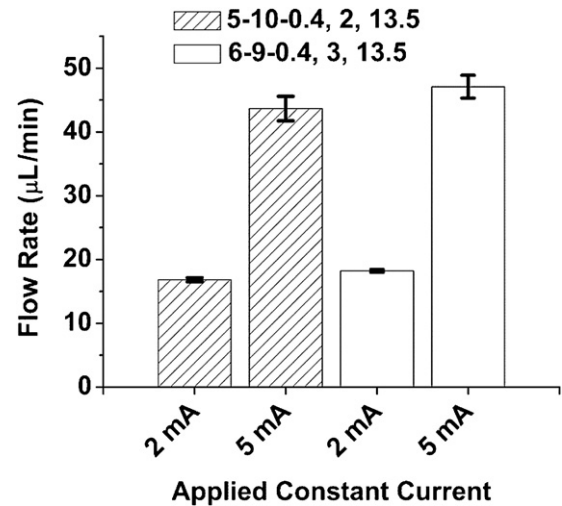
Bellows were loaded (1 bellows per design) until bursting, which occurred at 65 kPa for some designs and over 100 kPa as shown in table 5. The bellows designs stretched significantly and were permanently deformed. Photographs of deformed bellows are shown in figure 15.

#### 5.4. Integration with electrochemical actuators

It was shown previously that increasing the convolution number from 1 to 2 did not have a significant effect on the flow rate when bellows were integrated with electrochemical actuators [21]. Here, two different bellows designs with varying inner and outer diameters were integrated with electrochemical actuators and tested in an acrylic reservoir. Flow rates generated by the two bellows electrochemical actuators at 2 and 5 mA applied constant current were not significantly different (figure 16;  $p > 0.05$ ).

## 6. Discussion

Linear bellows equations and thin membrane approximations are not applicable for our Parylene C bellows, but with finite element models and simulations, deflection was approximated for several bellows designs. Load–deflection curves from



**Figure 16.** Flow rates (Mean  $\pm$  SE,  $n = 3$ ) generated by electrochemical actuators with bellows of two different designs (5 mm ID, 10 mm OD, 0.4 mm  $H$ , 2 convolutions, 13.5  $\mu\text{m}$  wall thickness; 6 mm ID, 9 mm OD, 0.4 mm  $H$ , 3 convolutions, 13.5  $\mu\text{m}$  wall thickness).

the nonlinear FEM simulations were comparable to the experimental results for 1 and 2 convolution bellows, but underestimated the deflection of 3 convolution bellows. The yield strength was not exceeded in the simulations of all three bellows designs, demonstrating operation within the elastic range for applied loads up to 3.45 kPa (0.50 psi). The bellows top surface was more dome like in benchtop testing than suggested by simulation results, indicating that FEM boundary conditions were too strict and underestimated the deflection at the edges of the topmost bellows convolution. Simulations achieved deflection approximations within 10% of the experimental load–deflection curve for 1 and 2 convolution designs above 2.76 kPa (0.30 psi) when the Young's modulus for Parylene was increased from 2.76 GPa to 4.75 GPa, but greatly underestimated center deflection for 3 convolution bellows.

Yang *et al* [3] argued that reduced rigidity provides significant improvement in deflection for a single convolution bellows over a flat diaphragm of the same material and dimensions. In [19], a Parylene C flat membrane of dimensions  $2.8 \times 1.6 \text{ mm}^2$  and thickness 2.8  $\mu\text{m}$  deflected only up to 65  $\mu\text{m}$  under 4 psi applied pressure. Flat and corrugated Parylene C diaphragms of dimensions  $4.3 \times 4.3 \text{ mm}^2$  achieved deflections of  $\sim 200 \mu\text{m}$  and  $< 50 \mu\text{m}$ , respectively, at 1.5 kPa [22]. Li *et al* simulated deflection of a Parylene bellows and corrugated diaphragm of approximately the same dimensions under the same load conditions (3.45 kPa applied pressure) and observed maximum deflections of 1.5 and 0.8 mm, respectively [11].

FEM simulations predicted stress exceeding the Young's modulus for Parylene C at  $\sim 5.52 \text{ kPa}$  (0.80 psi), which was similar to the value seen for plastic deformation in mechanical testing. The simulations also showed greater stress along the right angle convolution edges, particularly in the lowest convolution near the clamping site. Incorporation of a convolution profile with rounded edges may reduce

stress concentration at these locations. Sites of high stress concentration identified by FEM simulation were highly correlated to sites of burst failure of fabricated bellows.

The fabrication process was relatively quick and used minimal resources. A large number of molds can be made for the initial fabrication steps, but the overall throughput of the process is limited by the manual stacking step. Automation or an improved method for stacking the PEG modules could further increase the fabrication process throughput. The sidewall profiles of this simple hole punching method are restricted to the smoothness obtained from the polished metal punches, and could be a factor in material performance. Improved mold forming technologies need to be explored for further improvement in mold surface quality.

Smaller ID/OD ratios and larger convolution depths (difference between outer and inner radius) may allow for greater achievable deflection of bellows on this size scale, particularly at higher pressures. Although a power analysis with our *t*-test parameters indicated that the studies were relatively low power, we were still able to detect significance in all but one design parameter, ID. Small changes in ID from 1 to 2 mm did not have a noticeable effect except at the highest pressure tested for the 2 mm case (3.45 kPa). In the case of 5–9–0.4 versus 6–9–0.4, the ID to OD ratio increases from 0.56 to 0.67 and in 5–10–0.4 versus 7–10–0.4, the increase is from 0.50 to 0.70. This suggests that larger ID or ID to OD ratio changes or possibly sample sizes are required to elucidate the effect on achievable deflection. We expected that increasing OD while keeping all other parameters constant would enhance mobility and allow for greater deflection of the bellows. This was confirmed in the load–deflection testing for the magnitude of dimension change tested and the difference between the two bellows designs (varying only OD) was statistically significant. Reducing layer height (*H*), and thus overall bellows height, produced a statistically significant difference in deflection for the dimension change tested, but the deflection change was relatively small compared to the reduction in *H* and would need to be evaluated in the context of a given application. The number of convolutions (*N*) were varied to evaluate the potential benefit of additional convolutions to increase potential deflection range, but was kept low to minimize the overall bellows height in consideration of minimizing dimensions for integration in low profile MEMS devices. For the design parameters evaluated in this work, the most effective way to increase bellows deflection was to increase outer diameter, increase the number of convolutions or decrease wall thickness (table 4). Modifying these parameters provided the greatest change in deflection while requiring relatively small changes in initial bellows volume under no load. Thus, there are several options for addressing the balance between mechanical strength and anticipated displacement volume requirements with the overall volume occupied by the bellows once integrated with a MEMS actuator or system.

The load–deflection curves showed hysteresis at lower applied pressure loads than that with Parylene flat membranes tested by Shih *et al* where ~28 kPa (~4 psi) was the onset of hysteresis. Time for mechanical relaxation between cycles (after dropping from 0.69 kPa to 0.00) was on the order of

10 to 20 min, which is in agreement with stress relaxation time constants reported in [23]. Dimpling was observed at approximately the onset of hysteresis in the loading–unloading cycle. This was likely due to compressive stresses that developed near the edge of the convolutions, as is seen in simply supported diaphragms [16].

Burst pressure testing indicated that the designs with larger convolution depths (table 5) tended to burst at lower loads, corresponding with the relatively larger deflection and higher associated stress. The pressure transducer's range was limited to (~100 kPa) which in turn limited investigation of some parameters (such as wall thickness) on mechanical strength. In addition, only one bellows was used for each destructive test so further studies with larger sample sizes and a transducer with greater range would be needed to evaluate the effects of design parameter changes with statistical significance.

Two different bellows designs integrated with electrochemical actuators showed a statistically insignificant difference in generated flow rate. It is important to note that the pressure testing and the flow rate testing setups were in different fluidic environments (air versus liquid), which may have contributed to the insignificant effect of the tested design parameter variations (number of convolutions, diameter) on flow rate. For pressure testing, bellows were clamped in an open test fixture and deflected in ambient air. Static pressure was applied at the previously described values. During flow rate testing pressure was continuously increasing via electrolysis within the bellows, resulting in dynamic pressure values. The bellows deflected against fluid (water) in the rigid reservoir and the coupled fluid column in the rigid cannula, which was open at one end. Further investigation of bellows design parameters and their effect on flow rate is warranted and will be examined in future work. An individual bellows electrochemical actuator was tested over 100 times (much greater than that required by our intended applications) without noticeable changes in performance when operated in the elastic range (up to 3.45 kPa). Large deflection was achieved under relatively low applied pressures (~kPa) compared with a bellows integrated with a thermopneumatic actuator [3] while consuming significantly less power (~mm with ~3 mW versus ~μm with ~720 mW).

## 7. Conclusion

We demonstrated a rapid, high-yield fabrication process for MEMS Parylene C bellows for large deflection applications. The fabricated thin film polymer bellows exhibited repeatable behavior under loading within the determined elastic range and bellows of same design demonstrated uniform load–deflection performance. FEM simulations provided approximations of load–deflection curves for several bellows designs. The onset of hysteresis for the Parylene C bellows structure (4.19 kPa or 0.60 psi) was determined in mechanical testing. Large deflection (~mm) was achieved under relatively low applied pressure (~kPa). Bellows design parameters were evaluated and it was found that convolution number, wall thickness and outer diameter had the greatest effect on load–deflection (axial

extension) performance for the bellows designs fabricated. Bellows were combined with interdigitated electrodes to form electrochemical actuators and fluid pumping under low power ( $\sim 3$  mW) was demonstrated. Several design parameters can be adjusted to achieve a desired magnitude of deflection while maintaining dimensions appropriate for incorporation with MEMS actuators and devices. The bellows offer complete separation of the electrolyte from the reservoir fluid when integrated with electrochemical actuators and could have applications in other actuators where a separation of the actuation fluids and mechanisms from other system chambers is necessary. When constructed with Parylene C, which boasts biocompatibility, inertness to a broad range of chemicals, and low permeability, bellows are poised to become an enabling technology for novel applications in MEMS actuators and microfluidic systems.

## Acknowledgments

This work was funded in part by a National Science Foundation Graduate Research Fellowship under grant no DGE-0937362 (HG) and the Wallace H Coulter Foundation Early Career Translational Research Award. The authors would like to thank Ms Roya Sheybani for supplying Nafion<sup>®</sup>-coated electrochemical actuators and Ms Diya Dwarakanath, Ms Heather Chen and Mr Jason Hoffman for their assistance with fabrication of bellows. The authors would also like to acknowledge Dr Donghai Zhu and members of the Biomedical Microsystems Laboratory for their assistance with this project.

## References

- [1] Wilson J F 1984 Mechanics of bellows: a critical survey *Int. J. Mech. Sci.* **26** 593–605
- [2] Di Giovanni M 1982 *Flat and Corrugated Diaphragm Design Handbook* (New York: Dekker)
- [3] Yang X, Tai Y-C and Ho C-M 1997 Micro bellow actuators *Proc. IEEE Int. Conf. TRANSDUCERS (Beijing)* pp 45–8
- [4] Minami K, Morishita H and Esashi M 1999 A bellows-shape electrostatic microactuator *Sensors Actuators A* **72** 269–76
- [5] Bonanomi G, Rebello K, Lebouitz K, Riviere C, Di Martino E, Vorp D and Zenati M A 2003 Microelectromechanical systems for endoscopic cardiac surgery *J. Thorac. Cardiovasc. Surg.* **126** 851–2
- [6] Feng G-H and Kim E S 2003 Universal concept for fabricating micron to millimeter sized 3-D parylene structures on rigid and flexible substrates *Proc. IEEE Int. Conf. Microelectromechanical Systems (MEMS) (Kyoto, Japan)* pp 594–7
- [7] Luharuka R, Wu C-F and Hesketh P J 2004 Design, fabrication, and testing of a near constant pressure fuel delivery system for miniature fuel cells *Sensors Actuators A* **112** 187–95
- [8] Liu H-Y, Pi X-T, Zhou C-W, Zheng X-L, Hou W-S and Wen Z-Y 2008 Design of site specific delivery capsule based on MEMS *Proc. IEEE Int. Conf. Nano/Micro Engineered and Molecular Systems (NEMS) (Sanya, Hainan Island)* pp 498–501
- [9] Takashima K, Noritsugu T, Rossiter J, Guo S and Mukai T 2011 Development of curved type pneumatic artificial rubber muscle using shape-memory polymer *Proc. SICE Annual Conf. on Instrumentation, Control, Information Technology and System Integration (Tokyo, Japan)* pp 1691–5
- [10] Shapiro Y, Wolf A and Gabor K 2011 Bi-bellows: pneumatic bending actuator *Sensors Actuators A* **167** 484–94
- [11] Li P-Y, Sheybani R, Gutierrez C, Kuo J T W and Meng E 2010 A Parylene bellows electrochemical actuator *J. Microelectromech. Syst.* **19** 215–28
- [12] Gensler H, Sheybani R, Li P-Y, Mann R L and Meng E 2012 An implantable MEMS micropump system for drug delivery in small animals *Biomed. Microdevices* **14** 483–96
- [13] Matsui S 2003 Three-dimensional nanostructure fabrication by focused-Ion-beam chemical vapor deposition *Proc. IEEE Int. Conf. TRANSDUCERS (Boston, USA)* pp 179–81
- [14] Gensler H *et al* 2010 Implantable MEMS drug delivery device for cancer radiation reduction *Proc. IEEE Int. Conf. Microelectromechanical Systems (MEMS) (Hong Kong, SAR, China)* pp 23–6
- [15] Gensler H, Sheybani R and Meng E 2011 Rapid non-lithography based fabrication process and characterization of Parylene C bellows for applications in MEMS electrochemical actuators *Proc. IEEE Int. Conf. TRANSDUCERS (Beijing, China)* pp 2347–50
- [16] Ugural A C 2009 *Stresses in Beams, Plates, and Shells* (Boca Raton, FL: CRC Press)
- [17] Metz P, Alici G and Spinks G M 2006 A finite element model for bending behaviour of conducting polymer electromechanical actuators *Sensors Actuators A* **130–131** 1–11
- [18] Kim K H, Yoon H J, Jeong O C and Yang S S 2005 Fabrication and test of a micro electromagnetic actuator *Sensors Actuators A* **117** 8–16
- [19] Shih C Y, Harder T A and Tai Y-C 2004 Yield strength of thin-film parylene-C *Microsyst. Technol.* **10** 407–11
- [20] Sheybani R and Meng E 2012 High efficiency MEMS electrochemical actuators and electrochemical impedance spectroscopy characterization *J. Microelectromech. Syst.* **2** 1197–208
- [21] Sheybani R, Gensler H and Meng E 2011 Rapid and repeated bolus drug delivery enabled by high efficiency electrochemical bellows actuators *Proc. IEEE Int. Conf. TRANSDUCERS (Beijing, China: IEEE)* pp 490–3
- [22] Sim W, Kim B, Choi B and Park J-O 2005 Theoretical and experimental studies on the parylene diaphragms for microdevices *Microsyst. Technol.* **11** 11–15
- [23] Lin J C-H, Lam G and Tai Y-C 2012 Viscoplasticity of parylene-C film at body temperature *Proc. IEEE Int. Conf. Microelectromechanical Systems (MEMS) (Paris, France: IEEE)* pp 476–9